Hindawi
Advances in Polymer Technology
Volume 2019, Article ID 9501593, 4 pages
https://doi.org/10.1155/2019/9501593

Research Article

Study on the Synthesize, Characterization, and Conductive Performance of Nickelzircomolybdnum Heteropoly Acid Salt with Keggin Structure

Zhihong Zhang ,[1] Baoying Wang,[1] Yijing Zhang,[1] Gehong Zhang,[1] and Yujing Wang[2]

[1]*School of Civil & Architecture Engineering, Xi'an Technological University, Shaanxi, China*
[2]*School of Materials & Chemical Engineering, Xi'an Technological University, Shaanxi, China*

Correspondence should be addressed to Zhihong Zhang; zhzhang0416@163.com

Received 16 August 2019; Accepted 14 November 2019; Published 29 December 2019

Guest Editor: Lin Tang

A novel heteropoly acid salt, $Na_6[Ni(Mo_{11}ZrO_{39})]\cdot 20H_2O$, has been synthesized by the means of acidification and adding the reactants into the solution step by step. The heteropoly compound was characterized by elemental analysis, TGA/DSC, infrared spectrum, ultraviolet spectrum, X-ray diffraction, and SEM. Its protonic conduction was measured by the means of the electrochemical impedance spectrum. The results showed that it belongs to the Keggin type, and its conductivity value was 1.23×10^{-2} S/cm at 23°C when the relative humidity was 60%, and the conductivity enhanced with the elevated temperature. Its proton conduction mechanism was in accordance with vehicle mechanism, and the activation energy was 27.82 kJ/mol.

1. Introduction

The heteropoly compounds include the heteropoly salts and heteropoly acids, which are a class of discrete, transition-metal-oxide cluster anion. They have been widely used in many fields, particularly in the catalytic field, pharmaceutical field, biological science, and materials science [1–4]. Recent work has revealed that the heteropoly compounds have a fine conductive property, whether they are in solution or in solid state, just like other protonic conductors, such as inorganic matter [5–8]. In this thesis, we report the synthesis, characterization, conductive property, and conduction mechanism of nickelzircomolybdnum heteropoly acid salt with Keggin-type $Na_6[Ni(Mo_{11}ZrO_{39})]\cdot 20H_2O$ (abbreviated as NiZrMo).

2. Experiment

The heteropoly acid salt, $Na_6[Ni(Mo_{11}ZrO_{39})]\cdot 20H_2O$ has been synthesized by the means of acidification and adding the reactants into the solution step by step according to the procedure described in our previous report [9]. 200 mL aqueous solution of sodium molybdate (10.65 g, 0.044 mol, $Na_2MoO_4\cdot 2H_2O$) was adjusted to pH~6.0 with acetic acid. Then 20 mL aqueous solution of zirconium oxychloride (0.72 g, 0.004 mol, $ZrOCl_2\cdot 8H_2O$) was added dropwise to 200 mL aqueous solution of sodium molybdate under stirring. When the white precipitate appeared, the solution was adjusted to pH~5.0 after continuous stirring for a period of time at 70°C until the solution clarified. And 20 mL aqueous solution of nickel chloride (0.96 g, 0.004 mol, $NiCl_2\cdot 6H_2O$) was added dropwise, refluxing for 1-2 h. The cooled solution was extracted by ethanol (50 mL). After the concentrated ethanol solution was dried in vacuum, the pale-green NiZrMo powder was obtained.

All chemicals were of analytical grade and used without further purification.

3. Results and Discussion

3.1. Elemental Analysis. The molar ratio of the elemental was measured by means of the SPECTRO GENESIS FES Inductively Coupled Plasma Atomic Emission Spectroscopy (ICP-AES). As shown in Table 1, the mole ratio of Ni : Zr : Mo is close to 1 : 1 : 11 (data in the brackets is theoretical), which indicates it belongs to the 1 : 1 : 11 series of heteropoly acid salt.

Table 1: Elemental analysis of the heteropoly acid salt.

HPS	Ni (%)	Zr (%)	Mo (%)	Ni : Zr : Mo
NiZrMo	2.48 (2.52)	3.86 (3.91)	45.02 (45.36)	1 : 1 : 11

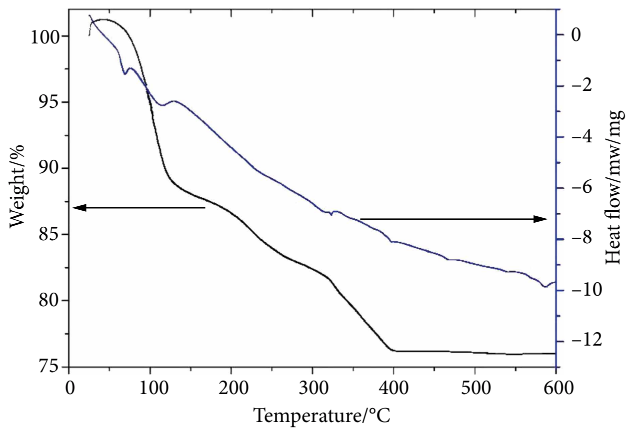

Figure 1: TGA/DSC curve of NiZrMo.

3.2. TGA/DSC Analysis. The thermogravimetric analysis (TGA) and differential scanning calorimetry (DSC) study was recorded on the METTLER TOLEDO thermal analyzer in a dynamic argon atmosphere from room temperature to 600°C, and the rate of heating was 15°C per minute. As shown in Figure 1, when the temperature increased from 74°C to 400°C, the weight of the heteropoly acid salt reduced; but the weight remains constant when the temperature exceeds over 400°C. There are four endothermic peaks, which are 74°C, 105°C, 325°C, and 400°C, in the DSC curve. The process can be divided into three major weight loss stages by these four peaks. At the first loss stage, the temperature from 74°C to 120°C, the total percent of weight loss is 9.5%, which is mainly comprised of physically absorbed water and acetic acid. In the second loss stage, the temperature from 120°C to 300°C, the lost weight is 9.3%, which corresponds to the loss of thirteen crystallized water molecules. In the third loss stage, the temperature from 300°C to 400°C, the lost weight is 5.0%, equivalent to the loss of seven crystallized water molecules. It is found that there are two endothermic peaks in the vicinity of 460°C and 575°C, which show the collapsed structure of NiZrMo. It can be concluded from Figure 1 that the accurate molecular formula of the product is $Na_6[Ni(Mo_{11}ZrO_{39})]\cdot 20H_2O$ and it remains constant within 400°C which shows its favorable thermal stability [10].

3.3. FT-IR and UV Analysis. The Fourier transform infrared (FT-IR) spectroscopy was carried out using a NICOLET NEXUS from the region of 600 cm^{-1} to 4000 cm^{-1} using KBr pellets. In the range of 700~1100 cm^{-1}, there were four characteristic vibrational bands of heteropoly acid salt with a Keggin structure. Figure 2 shows four characteristic bands respectively at 1020 cm^{-1} (Zr-Oa), 945 cm^{-1} (Mo=Od), 885 cm^{-1} (Mo-Ob-Mo), and 771 cm^{-1} (Mo-Oc-Mo) (among them Oa = oxygen in the central ZrO_4 tetrahedron, Od = terminal oxygen bonding to a Mo atom, Ob = edge-sharing oxygen connecting Mo atoms, and Oc = corner-sharing connecting Mo_3O_{18} units), all of which can be detected from a Keggin anion. Moreover, besides, the bond at 906 cm^{-1} is ascribed to the symmetric stretching of Mo=Od bonds, and the band at 1420 cm^{-1} could be ascribed to the stretchifvng vibration of C–O bonds or in -plane bending vibration of O–H bonds. In the region of high frequency, the bond at 1350 cm^{-1} might be attributed to the bending vibration of the C–H bonds. Besides, the band at 1560 cm^{-1} could be attributed to a carbonyl group. Meanwhile, there are two other bands at 1640 cm^{-1} and 3430 cm^{-1}, which are attributed to the bending vibration of the O–H bonds and the stretching vibration of the H–O–H bonds of absorbed water respectively [11]. The bands of a carboxyl group and C–H band is ascribed to the residue of the glacial acetic acid or its salts. Because the size of the zirconium ions is large, the stretching vibration band split, which may cause the relaxation and small cohesion of the molecule, so it is obvious that the relative chemical bond vibrations would change.

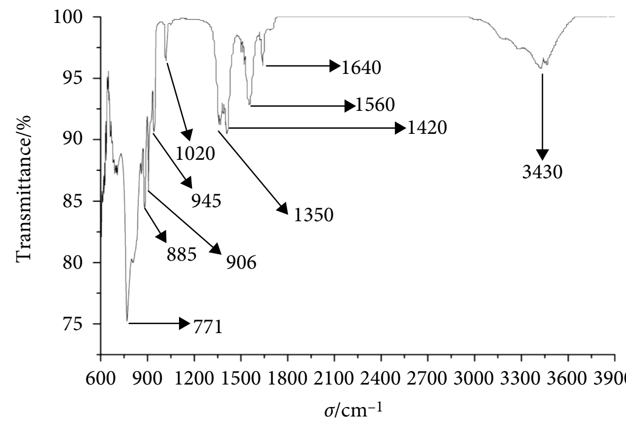

Figure 2: FT-IR spectrum of NiZrMo.

The ultraviolet (UV) spectrum was recorded on a SHIMADZU UV-2500 spectrophotometer with a wavelength range of 200~400 nm. The UV spectra of the 1 : 1 : 11 series of heteropoly acid (salts) of Keggin structure usually possess two strongly characteristic absorption peaks, the higher energy of the absorption peak is attributed to the double bond character, which is close to 200 nm, and the lower energy of the absorption peak is a result of the single bond character, which is in the vicinity of 250 nm.There are two peaks at 209 nm and 245 nm as show in Figure 3. They are attributed to the Od→Mo and Ob/Oc→Mo charge transfers respectively and both of them are in accordance with the typical absorption of the UV spectra of the 1 : 1 : 11 series of the Keggin structure heteropoly compounds.

3.4. XRD and SEM Analyses. X-ray powder diffraction (XRD) analysis was measured on a SHIMADZU XRD-6000 X-ray diffractometer. The instrument was equipped with Cu tube operated at 40 kV and 30 Ma, and the diffraction data collection was in the range of 5~40° 2θ with a step size of 0.02 at a rate of 4° per minute. Four characteristic peaks can be observed: 7~13°, 16~23°, 25~30°, and 31~38° in the XRD pattern of a 1 : 1 : 11 series of Keggin type heteropoly acid (salt). Figure 4 depicts the XRD pattern of the NiZrMo, there are four

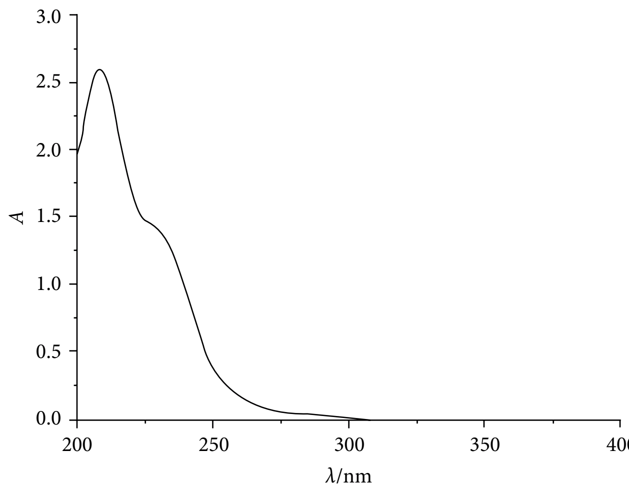

FIGURE 3: UV absorption spectrum of NiZrMo.

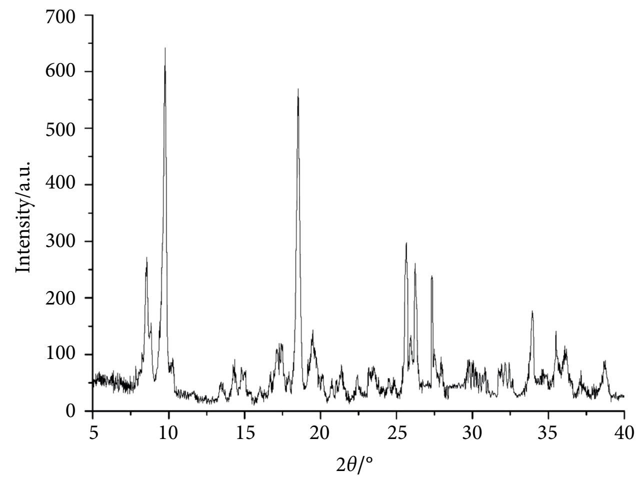

FIGURE 4: XRD pattern of NiZrMo.

characteristic peaks, which are 9.76°, 18.5°, 27.38°, and 33.98°, consistent with the characteristic peaks for the 1 : 1 : 11 series of Keggin structure heteropoly compound [12].

The surface morphology of the NiZrMo was performed using a KY-AMRAY 1000B scanning electron microscope (SEM) (Figures 5(a) and 5(b)). Figure 5 shows that heteropoly acid presents a honeycomb structure at low magnification and regular hexahedron shapes at high magnification. Although the heteropoly acid is different in size, but the shape is almost the same. In addition, it can be clearly seen that the size is basically just about 3 μm as presented.

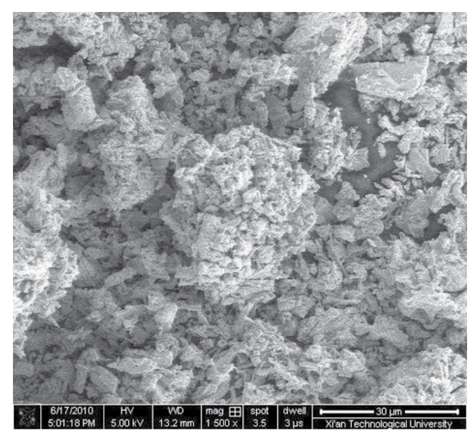

(a)

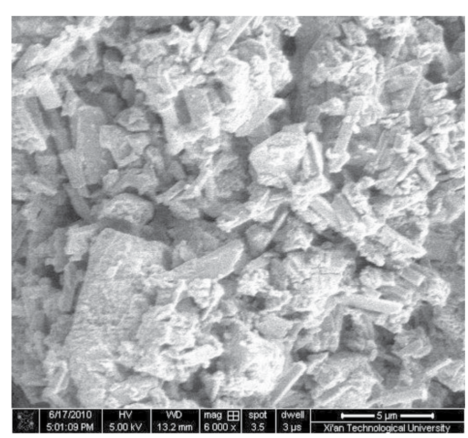

(b)

FIGURE 5: SEM images of the NiZrMo: low magnification and high magnification.

3.5. Electrochemical Impedance Spectrum Analysis. Impedance measurements of the NiZrMo were obtained using a VMP2 Multichannel potentiostat electrochemical impedance analyzer over a frequency range of $0.01{\sim}9.99 \times 10^4$ Hz at room temperature.

Figure 6 showed the electrochemical impedance spectrum (EIS) of NiZrMo. Proton conductivity of the heteropoly compound is calculated according to the relation, $\sigma = L/(S \times R)$, where R is the resistance, L is the thickness, and S is the area of the tablet [13]. From Figure 6, it is calculated that the proton conductivity of the NiZrMo is 1.23×10^{-2} S·cm^{-2} at temperature 23°C and 60% relative humidity. In the measurement temperature range, its proton conductivity increases with increasing temperature. The activation energy of proton conduction of NiZrMo is 27.82 kJ·mol^{-1}. The relationship between proton conductivity and activation energy is consistent to Arrhenius equation. The Arrhenius plot of proton conduction of NiZrMo is shown in Figure 6. Actually, there are two predominant mechanisms of proton conduction, which are in the Grotthuss mechanism, proton transport can be assisted by a large amount of water through a hydrogen-bonded network. There are differences between the Vehicle mechanism and the Grotthuss mechanism, in the later the proton movement was assisted by water molecule by means of facilitating transport as an H_3O^+ species. In addition, the activation energy of the Grotthuss mechanism is lower than that of the Vehicle mechanism, and the former is less than 15 kJ·mol^{-1}, the latter is more than 20 kJ·mol^{-1} [14]. So, the mechanism of proton conduction of NiZiMo is Vehicle mechanism for its activation energy is more than 20 kJ·mol^{-1}.

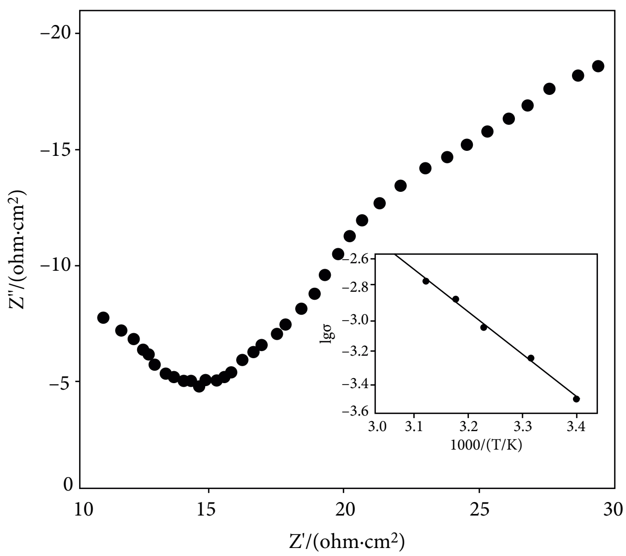

FIGURE 6: Electrochemical impedance spectrum of NiZrMo. Inset: arrhenius plot of conductivity for NiZrMo.

4. Conclusion

In our paper, a novel heteropoly acid salt with Keggin structure, $Na_6[Ni(Mo_{11}ZrO_{39})]\cdot 20H_2O$ was prepared and characterized, and its conductive performance was studied.

The element analysis shows that the molar ratio of the Ni : Mo : Zr is 1 : 11 : 1. The FT-IR spectroscopy, UV spectroscopy, and XRD patterns indicate that it possesses Keggin structure. In addition, XRD pattern shows that it has a regular hexagonal structure. The compound has high proton conductivity. The mechanism of proton conduction of $Na_6[Ni(Mo_{11}ZrO_{39})]\cdot 20H_2O$ is Vehicle mechanism.

Data Availability

The data used to support the findings of this study are available from the corresponding author upon request.

Conflicts of Interest

The authors declare that they have no conflicts of interest regarding the publication of this paper.

Acknowledgments

This work is financially supported by the National Natural Science Foundation of China (51508435) and the Foundation of Key Laboratory of Education Department of Shaanxi Province of China (16JS045).

References

[1] A. Muhammad, S. Jiang, and S. F. Ji, “Heteropoly acid encapsulated into zeolite imidazolate framework (ZIF-67) cage as an efficient heterogeneous catalyst for Friedel-Crafts acylation,” *Journal of Solid State Chemistry*, vol. 157, pp. 109–111, 2015.

[2] J. S. Yan, L. M. Ai, Q. Wang, Z. Q. Wang, E. Yong-Sheng, and H. B. Liu, “Synthesis, characterization and esterification application of acid-functionalized ternary heteropoly anion-based ionic liquids with temperature-responsive behavior,” *Chinese Journal of Inorganic Chemistry*, vol. 34, no. 12, pp. 2179–2187, 2018.

[3] H. Zhang, A. J. Xie, Y. H. Shen, L. G. Qiu, and X. Y. Tian, “Layer-by-layer inkjet printing of fabricating reduced graphene-polyoxometalate composite film for chemical sensor,” *Physical Chemistry Chemical Physics*, vol. 14, no. 37, pp. 12757–12763, 2012.

[4] C. Zhang, D. Tian, X. H. Yi et al., “Occurrence, distribution and seasonal variation of five neonicotinoid insecticides in surface water and sediment of the pearl rivers, South China,” *Chemosphere*, vol. 217, pp. 437–446, 2019.

[5] B. El Bakkali, G. Trautwein, J. Alcanic-Monge, and S. Reinoso, “Zirconia-supported 11-molybdovanadophosphoric acid: effect of the preparation method on their catalytic activity and selectivity,” *Acta Crystallographica Section-Structural Chemistry*, vol. 74, no. 11, pp. 1334–1347, 2018.

[6] J. Miao, Y. W. Liu, Q. Tang, D. F. He, G. C. Yang, and Z. Shi, “Proton conductive watery channels constructed by Anderson polyanions and lanthanide coordination cations,” *Dalton Transactions*, vol. 43, no. 39, pp. 12757–12763, 2014.

[7] L. Chen, X. J. Sang, J. S. Li et al., “The photovoltaic performance of dye-sensitized solar cells enhanced by using Dawson-type heteropolyacid and heteropoly blue-TiO2 composite films as photoanode,” *Inorganic Chemistry Communications*, vol. 38, pp. 78–82, 2013.

[8] X. H. Yi, C. Zhang, H. B. Liu et al., “Occurrence and distribution of neonicotinoid insecticides in surface water and sediment of the Guangzhou section of the Pearl River South China,” *Environmental Pollution*, vol. 251, pp. 892–900, 2019.

[9] Z. H. Zhang, Z. P. Liao, and G. H. Zhang, “Degradation performance of Keggin type Zn-Mo-Zr catalyst for acidic green B with ultrasonic wave,” *RSC Advances*, vol. 5, no. 77, pp. 63104–63110, 2015.

[10] M. L. Wei, Y. X. Wang, and X. J. Wang, “Two proton-conductive hybrids based on 2-(3-pyridyl) benzimidazole molecules and Keggin-type heteropolyacids,” *Journal of Solid State Chemistry*, vol. 209, pp. 29–36, 2014.

[11] C. N. Kato, K. Hara, A. Hatano, K. Goto, T. Kuribayashi, and K. Hayashi, “A Dawson-type dirhenium(V)-oxido-bridged polyoxotungstate: X-ray crystal structure and hydrogen evolution from water vapor under visible light irradiation,” *European Journal of Inorganic Chemistry*, vol. 2008, no. 20, pp. 3134–3141, 2008.

[12] M. J. Zhang, P. P. Zhao, Y. Leng, G. J. Chen, J. Wang, and J. Huang, “Schitt base structured acid-base cooperative dual sites in an ionic solid catalyst lead to efficient heterogeneous knoevenages condensations,” *Chemistry – A European Journal*, vol. 18, pp. 12773–12782, 2012.

[13] X. F. Wu, H. X. Cai, Q. Y. Wu, and W. F. Yan, “Synthesis and high proton conductive performance of vanadium-substituted Dawson structure heteropoly acid $H_8P_2W_{16}V_2O_{62}\cdot 20H_2O$,” *Materials Letters*, vol. 181, pp. 1–3, 2016.

[14] Y. W. Liu, X. Yang, J. Miao et al., “Polyoxometalate-functionalized metal-organic frameworks with improved water retention and uniform proton-conduction pathways in three orthogonal directions,” *Chemical Communications*, vol. 50, no. 70, pp. 10023–10026, 2014.